

Simulation and analysis of gas hydrate flow in pipeline with groove structure

Xin Ma ^{1, a}, Qi Yu ^{1, b}, Cairong Fan² and Shaowei Chen³

¹School of Mechanical and Electrical Engineering, Southwest Petroleum University 610500, China

²South China Natural Gas Sales Center, SINOPEC Natural Gas Company 510250, China

³Research Institute of Safety and Environmental Protection Quality Supervision and Inspection, CNPC Chuanqing Drilling Engineering Co., Ltd., 618300, China

Abstract

In the process of vertical pipeline transportation of natural gas hydrate, there are problems of particle accumulation and low transportation efficiency. Combined with the drag reduction effect of shark scales, the bionics principle was adopted to place a small groove structure which can reduce the fluid resistance in the pipe. FLUENT was used to study the flow distribution of hydrate in the vertical groove pipe and the change of pipeline transportation efficiency. The results show that the volume fraction of hydrate particles reaches the maximum value at the inlet of the pipeline, and the volume fraction of hydrate particles decreases toward the outlet, and the particles uniformly converge toward the center of the pipeline. The particle velocity in the central area of the pipe is the largest, and the velocity at the outlet is as much as twice the inlet velocity. The velocity near the wall of the pipe is very small, and there is almost no flow. Compared with the existing smooth pipeline, the efficiency of the system is increased by 3.92%. The pipe with groove structure can reduce the pressure drop in the pipeline, reduce the impact of fluid on the pipeline, reduce the total resistance and transport loss in the pipeline, and improve the efficiency of the pipeline system to a certain extent.

Keywords

Groove structure; gas hydrate; vertical hard pipe; the numerical simulation.

1. Introduction

In 2017, Chinese scientists discovered the hydrate deposited on the seabed in the South China Sea for the first time^[1]. Due to its special properties and location, it is difficult to adopt traditional mining methods, and generally adopt solid fluidization mining method^[2-4]. However, the problem of hydrate particle deposition in fluidization extraction process could not be solved well, resulting in low transportation efficiency.

Sharks that swim fast in the ocean are covered with special tiny scales that reduce drag. Combined with the bionics principle, the special scale structure is simplified into groove structure. Compared with smooth surface, groove structure has excellent drag reduction effect. At present, few people in this field combine gas hydrate transportation with fin drag reduction. Bechert^[5] used a test plate with rib structure for pipeline drag reduction test experiment. The results show that the rib structure can reduce the wall shear stress by 7.3% compared with the smooth pipe. Xu Hailiang^[6] determined the particle size, inner diameter, slurry transport speed and slurry transport volume fraction of the vertical riser pipe of NGH. Zhou Shouwei^[7-10] studied the transportation of hydrate by annular pipe, and the

hydrate was broken through drilling fluid into the internal drill pipe and then returned to the surface through annular pipe.

Therefore, combined with the mechanism of gas hydrate pipeline transportation and trench drag reduction, this paper studies its drag reduction effect.

2. Hydraulic conveying parameters of vertical riser

Pipe diameter D can be calculated according to the volume flow Q and slurry flow rate Vm of the system:

$$D = \sqrt{\frac{4Q}{\pi V_m}}$$

In order to make the slurry particles upward from the vertical pipe conveying, existing in the slurry must be greater than the velocity of particles sedimentation rate, but considering the hydrate particles in the process of the hydraulic conveying the moderating effect of environment factors such as earthquake and waves, so in order to guarantee the reliability of the system, slurry transportation speed is generally for the settling velocity of 3 ~ 4 times^[11].

$$\omega = \sqrt{\frac{4dg (\rho_s - \rho_w)}{3 C_D \rho_w}}$$

Where:d--particle size,m; G--Acceleration of gravity, 9.81m/s²; ρ_s-- mineral particle density, kg/m³; ρ_w -- seawater density,1040 kg/m³; C_D-- Resistance coefficient, 0.44;

Slurry transport speed must be greater than the critical velocity Vc^[12]

$$V_c = F_1 \sqrt{2gD \left(\frac{\rho_s - \rho_w}{\rho_w} \right)}$$

Where: F1--empirical coefficient related to particle volume fraction and diameter, take 1.33.

It is assumed that the density of pure gas hydrate is 930 kg/m³.The density of seafloor sediment is 1450 kg/m³;The density ρ_s of minerals with 50% mixed volume fraction is 1190 kg/m³^[13].The initial flow of the selected system was 420 m³/ h;According to the pipe diameter D is 300m, the slurry velocity Vm is 1.65m/s.

Combined with the research conclusions of relevant parameters of smooth vertical hard tube^[6], the following parameters are determined:

Table 1 The basic parameters

The sea	Density	1030kg/m ³
	Viscosity	1.8579kg/(m-s)
Hydrates	Density	1190kg/m ³
	Viscosity	12.1024kg/(m-s)
	Diameter	10mm
	Volume fraction	25%
Pipe	Diameter	300mm
Slurry	Velocity	1.65m/s
Groove	Tooth width S	1mm
	Depth H	1mm

3. Mathematical Model

3.1. The basic assumptions

Solid-liquid phase is an incompressible continuous fluid, and the physical properties of each phase are constant. Main phase is seawater, secondary phase is gas hydrate particles; NGH particles are spherical particles with uniform particle size and no phase transformation, and the interphase heat transfer problem is not considered.

3.2. The governing equation

Euler model is used. The transient N-S equation was averaged by Reynolds and the governing equation in time-mean form was obtained [14].

The continuity equation is:

$$\frac{\partial \rho}{\partial t} + \frac{\partial}{\partial x_i} (\rho u_i) = 0$$

The momentum equation is:

$$\frac{\partial (\rho u_i)}{\partial t} + \frac{\partial}{\partial x_j} (\rho u_i u_j) = -\frac{\partial p}{\partial x_i} + \frac{\partial}{\partial x_j} (\mu \frac{\partial u_i}{\partial x_j}) + \frac{\partial \tau_{ij}}{\partial x_j}$$

Where, ρ -- liquid phase density, kg/m³;

T -- for time, s;

U_i, U_j -- velocity component, m/s;

X_i, X_j -- x and y coordinates, m;

P -- Pressure, Pa;

μ -- Dynamic viscosity, Pa·s;

$\tau_{ij} = -\rho U_i' U_j'$ -- Reynolds stress, where U_i' and U_j' are the pulsations of corresponding U_i and U_j .

3.3. The turbulence model

The standard k- ϵ model provided by FLUENT software is adopted, and the corresponding transport equation is [15-16].

3.4. Meshing

A model pipe with a length of 10 m is used as the simulation object to divide the pipe into 987600 units of THREE-DIMENSIONAL structural grid, and the grid around the pipe wall is encrypted, as shown in Figure 1. The enlarged image of the pipe edge is shown in Figure 2.



Fig. 1 3D structure grid of model pipes Fig. 2 Enlarged view of grid edge of pipe

3.5. The boundary conditions

In this paper, the SIMPLE algorithm is used to discretely solve the first-order upwind scheme difference equation, and the algebraic equation iterative calculation adopts subrelaxation, and the convergence accuracy is set as 10^{-3} .

1) Define the inlet boundary condition as the velocity inlet, the velocity is the slurry conveying velocity, and the velocity direction is vertical upward, considering the influence of gravity.

2) The outlet boundary condition is defined as the pressure outlet, and the outlet pressure, turbulence intensity and hydraulic diameter are given.

3) Non-slip solid wall boundary conditions are adopted for the wall surface, and environmental factors such as gravitational acceleration are applied.

4. Simulation results and analysis

4.1. Distribution of particles in vertical pipes

Particle diameter $D = 10\text{mm}$ is used, and particle distribution cloud map is shown in Figure 4. According to the comparison between smooth pipe and grooved pipe in FIG. 3(a) and (b), particles of the pipes in both cases were accumulated to varying degrees near the entrance, and there was no blockage in both cases. As the pipe develops, the volume fraction of the particles gets smaller. In the smooth pipe, the volume fraction reaches the highest (55%) at 1/3 of the pipe, and then decreases slightly. At the exit, most of the volume fraction is in the range of 30%-45% except for the high volume fraction at the pipe center, and the lower the volume fraction is closer to the pipe wall. There is almost no slurry distribution or only a thin layer of slurry at the wall of the tube. Pipeline with grooves also appear similar phenomenon, but unlike smooth pipe, pipe inlet with grooves on the volume fraction is bigger than smooth tube volume fraction, and, by the development of fluid volume fraction linearly reduce, not smooth the central part of the pipeline of high volume fraction, and the closer the export pipeline, pipe wall at low volume fraction slurry in pipe accounts for more than, The volume fraction of the central section is lower than that of the pipe inlet.

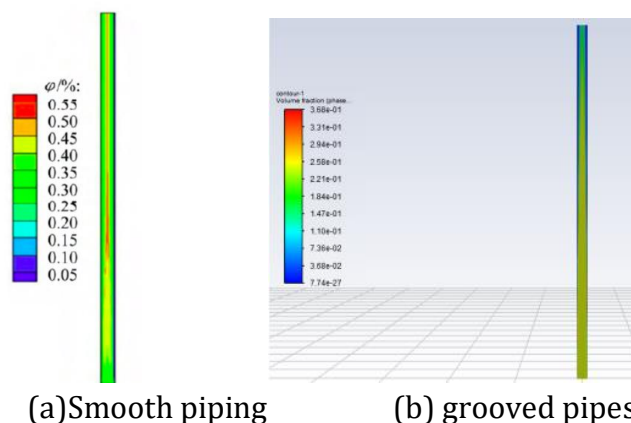


FIG. 3 Cloud map of particle distribution in pipeline

4.2. Distribution of slurry velocity in vertical pipe

FIG. 4 shows the velocity cloud diagram of smooth pipe outlet section, and FIG. 5 shows the velocity cloud diagram of grooved pipe outlet section. The comparison between FIG. 4 and FIG. 6 shows that in vertical pipes, the maximum flow velocity is in the center of the pipe. The maximum flow velocity in smooth pipes is slightly higher than that in slurry inlet, and the maximum flow velocity in grooved pipes is far higher than that in slurry inlet, even more than twice that in slurry inlet. The flow rate decreases radially from the central region and approaches 0 m/s at the tube wall. Due to the 1mm triangular fins on the surface of the trench pipe, the low-velocity area near the wall is thicker than that on the smooth pipe surface. The "secondary vortex phenomenon" will occur on the trench surface, that is, whirlpool will appear inside the trench, and the swirl will rotate in the same direction as the flow direction of the slurry, which will reduce the fluid resistance. At the same time, hydrate particles may fill up the surface of the groove and roll in the groove, and at the same time roll with other particles to accelerate the flow, so that the velocity at the outlet end is twice as much as that at the inlet end.

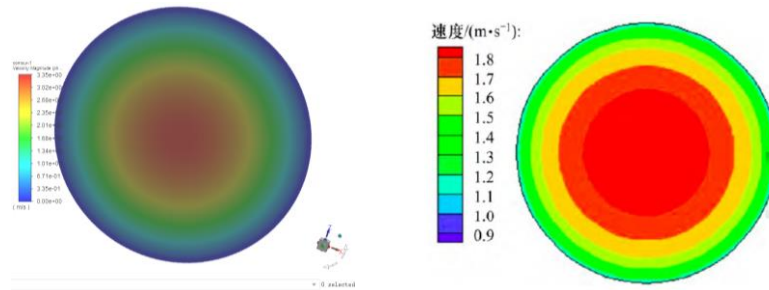


FIG. 4 Velocity cloud of channel outlet section FIG. 5 Velocity of smooth pipe outlet section

4.3. Calculation and analysis of pipeline pressure and transportation efficiency

The above qualitative analysis cannot quantitatively calculate the influence of the two pipelines on the conveying system, so the analysis must be carried out from the aspects of pipeline pressure drop, pressure loss, resistance loss and efficiency.

Calculate the pressure drop of the model pipeline:

$$P_c = P_{in} - P_{out}$$

Where: P_c -- pressure drop of pipeline, Pa;

P_{in} -- Pressure at inlet of pipe, Pa;

P_{out} -- outlet pressure of pipe, Pa.

Calculate the pressure loss of the model pipeline:

$$P_s = P_c - \rho_w g h_0$$

Where: P_s -- pipeline pressure loss, Pa;

H_0 -- Length of model pipe, 10 m.

Calculate the resistance loss of the model pipeline:

$$P_y = P_c - \rho_m g h_0$$

Where: P_y -- pipeline resistance loss;

ρ_m -- Slurry density, kg/m³.

4) Pressure prediction of system vertical grooved pipe:

The flow rate of slurry in this system is not high, and the distribution of total pressure along the pipeline can be regarded as a linear distribution, so the pressure drop, pressure loss and resistance loss of the model pipeline can be used to predict the corresponding value of the system (i.e., the whole length of 4 km).

$$P_{xz} = \frac{h}{h_0} P_x$$

Where: P_{xz} stands for P_{cz} , P_{sz} and P_{yz} , namely, the total pressure drop, total pressure loss and total resistance loss of the system, Pa;

H -- the depth of the sea, m.

System transport efficiency: The total pressure loss and total resistance loss can be used to calculate the system efficiency:

$$\eta = (1 - \frac{P_{yz}}{P_{sz}}) \times 100\%$$

4.3.1. Influence of slurry velocity on system efficiency

The optimized particle size, volume fraction, slurry flow rate and mineral density of Xu Hailiang et al.[6] were used to compare the results of groove structure and smooth structure on the basis of them, as shown in Table 2.

Table 2 Influence of slurry velocity on calculating model pipe pressure

Type	Pin/kPa	Pout/kPa	Pc/kPa	Py/kPa	Ps/kPa
Smooth	1.3704	-104.6769	106.0473	0.3446	4.0233
With grooves	1.2054	-104.6769	105.8823	0.1796	3.8583

Table 3 Influence of slurry velocity on system efficiency

Type	Vm/(m.s-1)	Pyz/kPa	Psz/MPa	η /%
Smooth	1.65	137.840	1.60932	91.43
With grooves	1.65	71.84	1.54332	95.35

The comparison shows that the pipeline with groove structure can reduce the pressure drop in the pipeline to a certain extent, reduce the impact of fluid on the pipeline, reduce the total resistance and transportation loss in the pipeline, and improve the efficiency of the pipeline system by 3.92%.

5. Conclusion

1) In smooth vertical lifting hard pipe and groove vertical lifting hard pipe of deep sea gas hydrate mining system, the distribution rule of hydrate particles is that the concentration near the entrance is high, and the concentration gradually decreases towards the outlet, and the particles tend to accumulate in the central area.

2) grooved pipe slurry velocity distribution at the center area is big, around two times than import slurry flow rate, flow velocity near the wall is small, close to 0 m/s, and as a result of the action of triangular fin, makes the "zero velocity is greater than the thickness of the smooth tube, can largely reduce the fluid flow resistance, in line with the principle of "secondary vortex";

3) To a certain extent, the pipeline with groove structure can reduce the pressure drop in the vertical transportation pipeline of natural gas hydrate, reduce the impact of fluid on the pipeline, reduce the total resistance and transportation loss in the pipeline, and improve the efficiency of the pipeline system.

References

- [1]. Editorial Department of Guangdong Shipbuilding. The first discovery of exposed "combustible ice" in south China sea in China [J]. Guangdong shipbuilding, 2017, 36(5): 99
- [2]. Siažik J & Malcho M. Accumulation of primary energy into natural gas hydrates [J]. Procedia Engineering, 2017, 192: 782-787.
- [3]. Song Yongchen, Yang Lei, Zhao Jiafei, Liu Weiguo, Yang Mingjun, Li Yanghui, et al. The status of natural gas hydrate research in China: A review [J]. Renewable & Sustainable Energy Reviews, 2014, 31(2): 778-791.
- [4]. Xu Chugang, Cai Jing, Lin Fuhua, Chen Zhaoyang & Li Xiaosen. Raman analysis on methane production from natural gas hydrate by carbon dioxide-methane replacement [J]. Energy, 2015, 79(19): 111-116.
- [5]. D.W. Bechert, M. Bruse, et al. Fluid Mechanics of Biological surface and Technological-Application. [J]. Naturwissenschaften. 2000, 87: 157-171.

- [6]. Hailiang Xu, Qiumin Xie, Bo Wu, Haiming Zhao, Shaojun Xu. Numerical simulation analysis of hydraulic lift of gas hydrate extraction pipeline [J]. Journal of Central South University (Science and Technology), 2015, 46(11): 4062–4069.
- [7]. Zhou Shouwei, Zhao Jinzhou, Li Qingping, Chen Wei, Zhou Jianliang, Wei Na, et al. Optimal design of the engineering parameters for the first global trial production of marine natural gas hydrates through solid fluidization [J]. Natural Gas Industry, 2017, 37(9): 1-14.
- [8]. Zhao Jinzhou, Zhou Shouwei, Zhang Liehui, Wu Kaisong, Guo Ping, Li Qingping, et al. The first global physical simulation experimental systems for the exploitation of marine natural gas hydrates through solid fluidization [J]. Natural Gas Industry, 2017, 37(9): 15-22.
- [9]. Wei Na, Sun Wantong, Meng Yingfeng, Zhou Shouwei, Fu Qiang, Guo Ping, et al. Annular phase behavior analysis during marine natural gas hydrate reservoir drilling [J]. Acta Petrolei Sinica, 2017, 38(6): 710-720.
- [10]. Gao Yonghai, Sun Baojiang, Zhao Xinxin, Wang Zhiyuan, Yin Zhiming & Wang Jinbo. Multiphase flow in wellbores and variation laws of the bottom hole pressure in gas hydrate drilling [J]. Acta Petrolei Sinica, 2012, 33(5): 881-886.
- [11]. Fei Xiangjun. Hydraulics of Slurry and Granular Material Handling [M]. Beijing: Tsinghua University Press, 1994: 74–79.
- [12]. Durand R. Hydraulic transport of coal and solid materials in pipes [C]// Proceedings of Colloquium on the Hydraulic Transport of Coal. London, 1952: 39–52.
- [13]. QU Kehui. Research of seabed gas hydrate hydraulic transportation based on the solid state mining [D]. Changsha: Central South University. School of Mechanical and Electrical Engineering, 2010: 4–16.
- [14]. [14] LI Wan, QIAN Zhongdong, GAO Yuanyong. Comparison of pressure oscillation characteristics in a Francis hydraulic turbine with four different turbulence models [J]. Engineering Journal of Wuhan University, 2013, 46(2): 174–179.
- [15]. QI Nana, ZHANG Hu, ZHANG Kai, et al. CFD simulation of particle suspension in a stirred tank [J]. Particuology, 2013, 11(3): 317–326.
- [16]. HU Jiehua, GU Zhengqi, HE Yibin, et al. Numerical simulation and experimental research on turbulent wake of vehicle [J]. Journal of System Simulation, 2010, 20(2): 321–325.